Supplementary Materials for

Loss of *UBE3A* impacts both neuronal and non-neuronal cells in human cerebral organoids

Authors

R. Chris Estridge[1,†] , Z. Begum Yagci[1,†], Dilara Sen[1,†], Tyler J. Johnson[1], Gautami R. Kelkar[1], Travis S. Ptacek[2], Jeremy M. Simon[2,3,4,5,*], Albert J. Keung[1,*]

Affiliations

[1]Department of Chemical and Biomolecular Engineering, North Carolina State University, Raleigh, NC, USA
[2]UNC Neuroscience Center, The University of North Carolina at Chapel Hill, Chapel Hill, NC, USA
[3]Department of Genetics, University of North Carolina Chapel Hill, Chapel Hill, NC, USA
[4]Department of Data Science, Dana-Farber Cancer Institute, Boston, MA, USA
[5]Department of Biostatistics, Harvard T. H. Chan School of Public Health, Boston, MA, USA
[†]These authors contributed equally.
[*] These authors jointly supervised this work.
Correspondence: jsimon@ds.dfci.harvard.edu; ajkeung@ncsu.edu

This PDF file includes:

Supplementary Figures S1 to S6
Supplementary Tables S1 to S3
Supplementary References (1 to 97)

Other Supplementary Materials for this manuscript include the following:

Supplementary Data 1 to 6

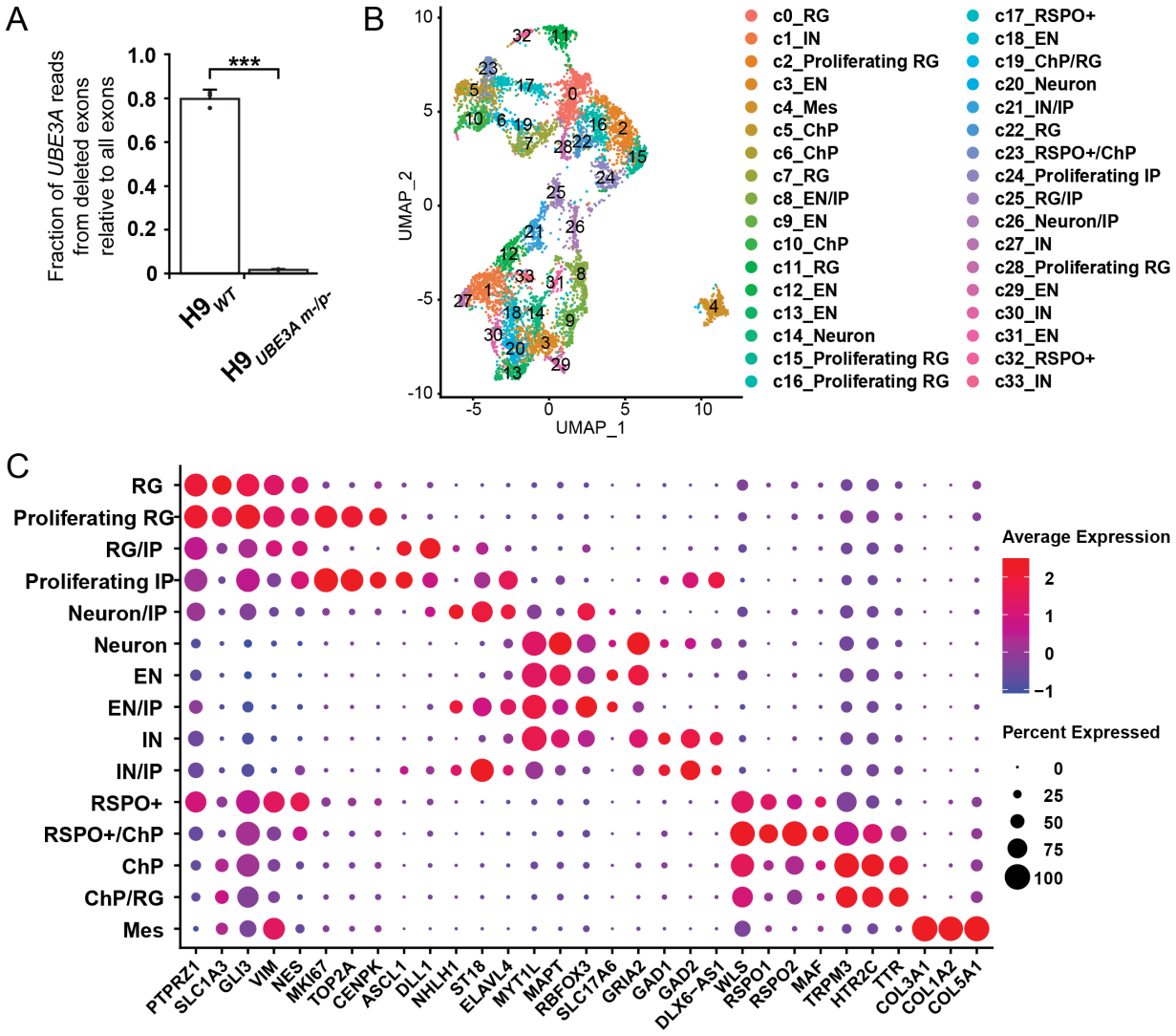

Supplementary Figure S1. Additional data from the scRNAseq experiment performed on 6 week organoids. Related to Figure 2.

(A) Fraction of *UBE3A* reads from deleted exons relative to all exons confirming the deletion in H9$_{UBE3A\ m-/p-}$ organoids. Coverage computed for each exon of *UBE3A* for each genotype and replicate for all cells. ***p-value <0.001, one-tailed t-test. n = 3 replicates of 4-5 pooled organoids per genotype. Error bars are 95% confidence intervals. (B) UMAP of 6 week H9$_{WT}$ and H9$_{UBE3A\ m-/p-}$ organoid cell cluster identities. RG: radial glia; IN: inhibitory-like neuron; EN: excitatory-like neuron; ChP: choroid plexus; IP: intermediate progenitor; Mes: Mesenchymal. (C) Cell type markers used to identify cell types. There were 15 broad cell types identified consisting of mainly radial glia (RG, e.g., *PTPRZ1*, *GLI3*, *SLC1A3*[1]), intermediate progenitors (IP, e.g., *ASCL1*[2] *NHLH1*[3,4]), mesenchymal cells (e.g., *COL3A1*, *COL1A2*[5]), choroid plexus (ChP, e.g., *TRPM3*, *TTR*[6]), RSPO+ cells (e.g., *RSPO1/2/3*[5]) and neurons (e.g., *MYT1L*, *DCX*[5]). Proliferating RG or IP clusters contained the cell cycle markers (e.g., *MKI67*, *TOP2A*[7]). The neurons containing excitatory (e.g., *SLC17A6*, *GRIA2*[4,8]) and inhibitory (e.g., *GAD1/2*[8,9]) markers were labeled as excitatory-like (EN) and inhibitory-like (IN) neurons, respectively.

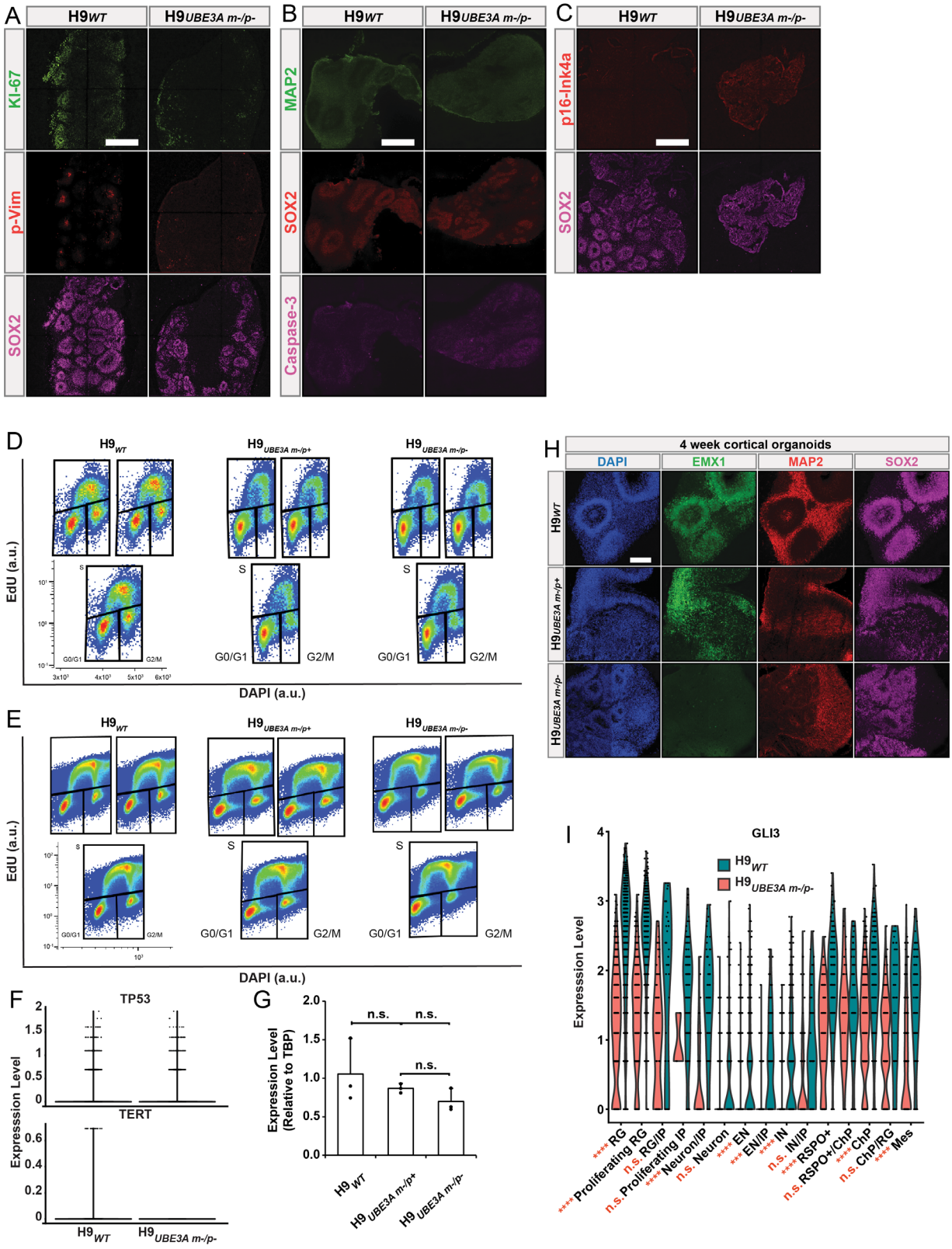

Supplementary Figure S2. Additional data regarding proliferation, apoptosis, senescence and corticogenesis. Related to Figure 4.

Immunostaining of H9$_{WT}$ and H9$_{UBE3A\ m-/p-}$ organoids with proliferation (Ki-67, A), apoptosis (Caspase-3, B) and senescence (p16-Ink4a, C) markers. Scale bars = 500 µm. Flow cytometry plots of EdU labeled H9$_{WT}$, H9$_{UBE3A\ m-/p+}$ and H9$_{UBE3A\ m-/p-}$ embryoid bodies (D) and pluripotent stem cells (E). (F) Violin plots of *TP53* and *TERT* expression levels for H9$_{WT}$ and H9$_{UBE3A\ m-/p-}$ organoids in

scRNAseq data. (G) RT-qPCR measurements of mRNA levels of *TERT* in H9$_{WT}$, H9$_{UBE3A\ m-/p+}$ and H9$_{UBE3A\ m-/p-}$ embryoid bodies normalized to *TBP*, relative to H9$_{WT}$ embryoid bodies. n.s. (not significant, p-value>0.05) via one-way ANOVA with Tukey-Kramer post hoc analysis, n = 3 replicates of ~110 pooled embryoid bodies per genotype. Full tick mark indicates sample being compared to half tick mark samples. Error bars are 95% confidence intervals. (H) Immunostaining of H9$_{WT}$, H9$_{UBE3A\ m-/p+}$ and H9$_{UBE3A\ m-/p-}$ human cortical organoids with EMX1, MAP2 and SOX2. Scale bars = 500 μm. (I) *GLI3* expression levels in H9$_{WT}$ and H9$_{UBE3A\ m-/p-}$ organoids in scRNAseq data. ***p-value<0.001, ****p-value<0.0001, n.s. (not significant, p-value>0.05). p-values were obtained from the DEG list. Please refer to Supplementary Data 1 to see the p-values. RG: radial glia; EN: excitatory-like neuron; IN: inhibitory-like neuron; ChP: choroid plexus; IP: intermediate progenitor; EN-CL: cortical layer-like neurons; Mes: mesenchymal; HSP: heat shock protein.

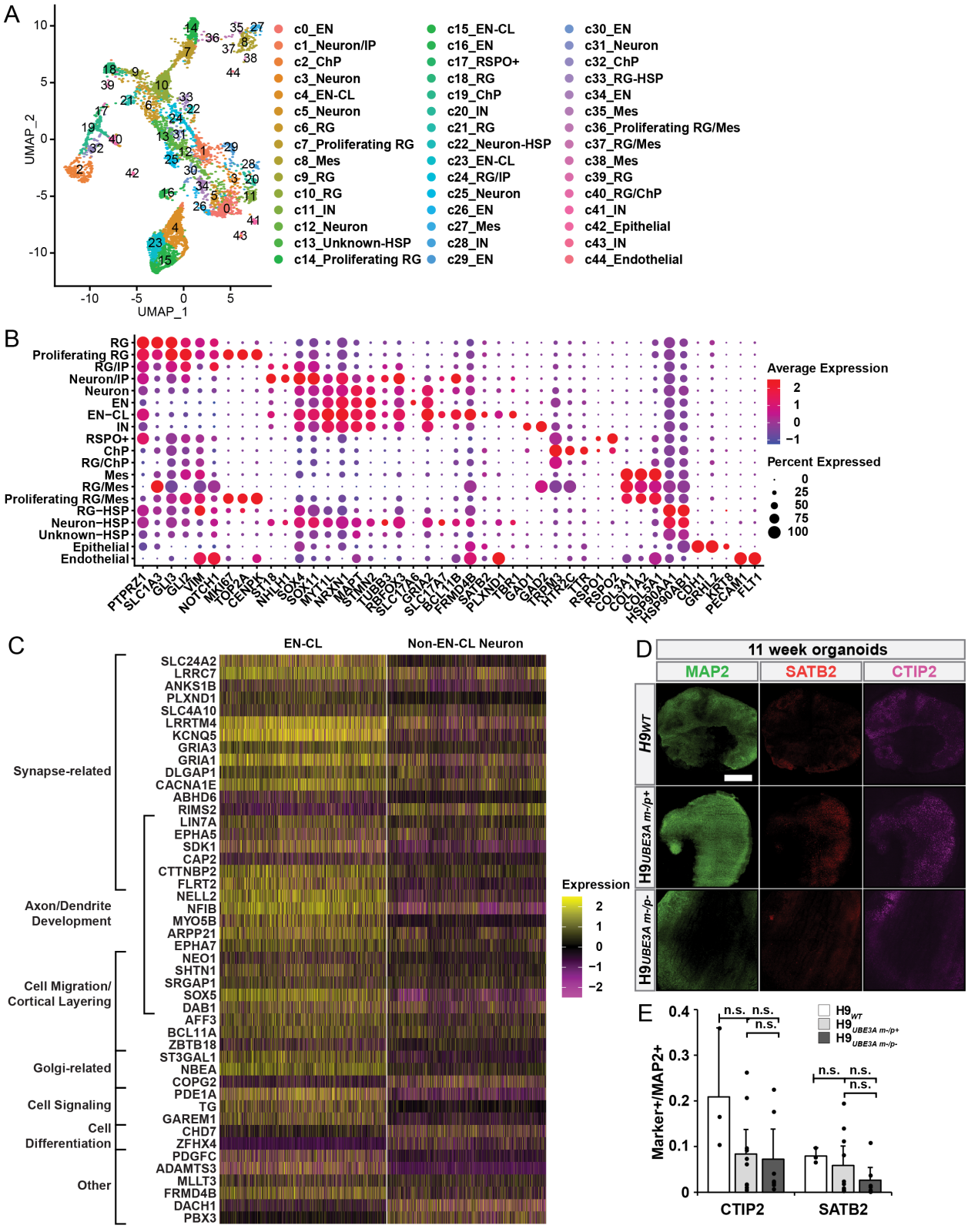

Supplementary Figure S3. Additional data from the scRNAseq experiment performed on 11 week organoids. Related to Figure 5.

UMAP of 11 week H9*WT* and H9*UBE3A m-/p-* organoid cell cluster identities. RG: radial glia; EN: excitatory-like neuron; IN: inhibitory-like neuron; ChP: choroid plexus; IP: intermediate progenitor; EN-CL: cortical layer-like neurons; Mes: mesenchymal; HSP: heat shock protein. (B) Cell type markers used to identify cell types. There were 18 cell types identified (excluding 1

unknown cell type) consisting of mainly radial glia (RG, e.g., *PTPRZ1*, *GLI3*, *SLC1A3*[1]), neuron/intermediate progenitors (neuron/IPs, e.g., *NHLH1*[3,4]), mesenchymal cells (e.g., *COL3A1*, *COL1A2*[5]), choroid plexus (ChP, e.g., *TRPM3*, *TTR*[6]), RSPO+ cells (e.g., *RSPO1/2/3*[5]) and neurons (e.g., *MYT1L*, *DCX*[5]). Proliferating RG or IP clusters contained the cell cycle markers (e.g., *MKI67*, *TOP2A*[7]). Neurons containing excitatory (e.g., *SLC17A6*, *GRIA2*[4,8]) and inhibitory (e.g., *GAD1/2*[8,9]) markers were labeled as excitatory-like (EN) and inhibitory-like (IN) neurons, respectively. Neurons with cortical layer neuron markers (e.g., *FRMD4B*, *SATB2*, *PLXND1*, *TBR1*[4,8,10–12]) were labeled as EN-CL. Clusters containing heat shock proteins (e.g., *HSP90AA1*, *HSP90AB1*) as top cluster markers were labeled as RG-HSP and Neuron-HSP depending on their marker gene list. There was one cluster unknown with HSPs being the top gene markers (Unknown-HSP). Two small clusters were labeled as epithelial (e.g., *KRT8*[13], *TJP1*[14]) and endothelial cells (e.g., *FLT1*, *PECAM1*[5]). (C) Heatmap of some of the top differentially expressed genes between EN-CL and non EN-CL neurons (EN, IN, Neuron, Neuron/IP, Neuron-HSP). Differentially expressed markers were grouped by cellular function: synapse-related (*SLC24A2*[15–19], *LRRC7*[20], *ANKS1B*[21], *PLXND1*[22], *SLC4A10*[23], *LRRTM4*[24], *KCNQ5*[25], *GRIA3*[16–19,26,27], *GRIA1*[28], *DLGAP1*[29], *CACNA1E*[16–19,30], *ABHD6*[31,32], *RIMS2*[33–36], *LIN7A*[37], *EPHA5*[38,39], *SDK1*[16–19,40–42], *CAP2*[43,44], *CTTNBP2*[45,46], *FLRT2*[16–19,47–49], *DAB1*[50–52], *NBEA*[16–19,53–56]), axon/dendrite development (*LIN7A*[37], *EPHA5*[38,39], *SDK1*[16–19,40–42], *CAP2*[43,44], *CTTNBP2*[45,46], *FLRT2*[16–19,47–49], *NELL2*[57], *NFIB*[58], *MYO5B*[59], *ARPP21*[60], *EPHA7*[61,62], *NEO1*[63], *SHTN1*[64–66], *SRGAP1*[67], *SOX5*[68], *DAB1*[50–52]), cell migration/cortical layering (*LIN7A*[37], *FLRT2*[16–19,47–49], *NEO1*[63], *SHTN1*[64–66], *SRGAP1*[67], *SOX5*[68], *DAB1*[50–52], *AFF3*[69], *BCL11A*[70], *ZBTB18*[71,72]), golgi-related (*ST3GAL1*[16–19,73], *NBEA*[16–19,53–56], *COPG2*[74]), cell signaling (*PDE1A*[16–19,53,75], *TG*[76], *GAREM1*[16–19,77,78]), cell differentiation (*CHD7*[79], *ZFHX4*[80]), and other (*PDGFC*[81,82], *ADAMTS3*[83], *MLLT3*[84], *FRMD4B*[85], *DACH1*[86], *PBX3*[87]). (D) Immunostaining of 11 week H9$_{WT}$, H9$_{UBE3A\ m-/p+}$ and H9$_{UBE3A\ m-/p-}$ organoids with CTIP2 and SATB2. Scale bars = 500 μm. (E) Immunostaining quantification for CTIP2 and SATB2 in 11 week H9$_{WT}$, H9$_{UBE3A\ m-/p+}$ and H9$_{UBE3A\ m-/p-}$ organoids. n.s. (not significant, p-value>0.05) via one-way ANOVA with Tukey-Kramer post hoc analysis, n ≥ 3 organoids per genotype. Full tick mark indicates sample being compared to half tick mark samples. Error bars are 95% confidence intervals.

Supplementary Figure S4. Summary. Related to Figures 1 to 7. Summary of the main results (A), and summary tables for the pathways for (B) 6 week and (C) 11 week scRNAseq data. The pathways shown are representative pathways for each category. Please refer to Supplementary Data 2 and 5 to see all the pathways. CH: Cellular Homeostasis, S: Senescence, T: Telomere-related, C: Circadian-related, CS: Cellular Stress, NA: Neuronal Activity. Figure S4A was created in https://BioRender.com.

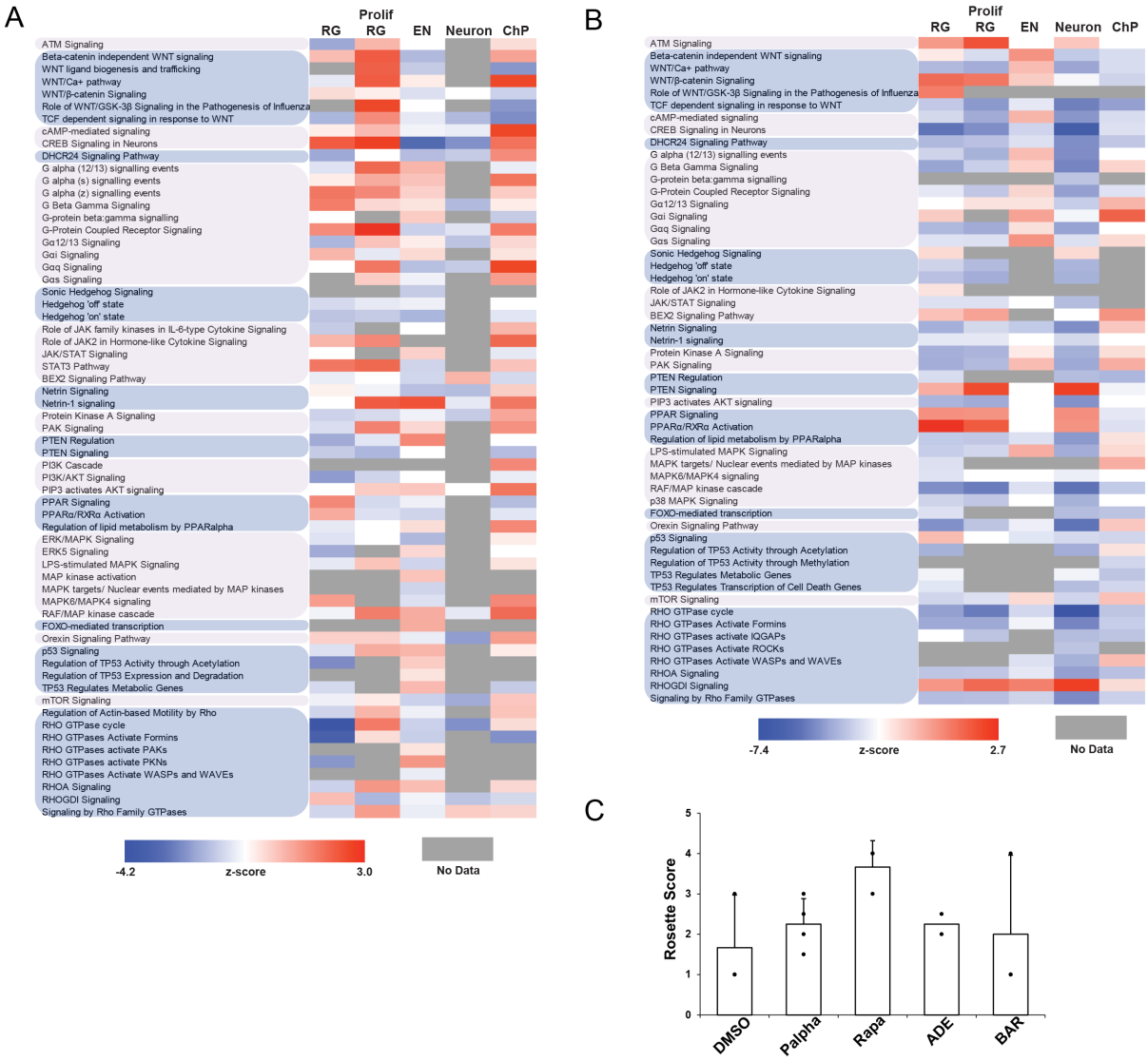

Supplementary Figure S5. Pathways identified to be directly or indirectly targeted in mechanistic and inhibitor studies. Related Figure 8. (A) 6 week scRNAseq pathway analysis. The pathways were organized broadly into groups. Please refer to Supplementary Data 2 to see all the pathways. (B) 11 week scRNAseq pathway analysis. The pathways were organized broadly into groups. Please refer to Supplementary Data 5 to see all the pathways. (C) Rosette structure scoring for the organoids treated with the vehicle control (DMSO) and the selected inhibitors. n≥3 organoids per condition with Adezmapimod 10μM being an exception with n=2. BAR: Baricitinib, ADE: Adezmapimod, Palpha: Pifithrin-α hydrobromide and Rapa: Rapamycin. Error bars are 95% confidence intervals. Error bars are not provided for samples with n<3.

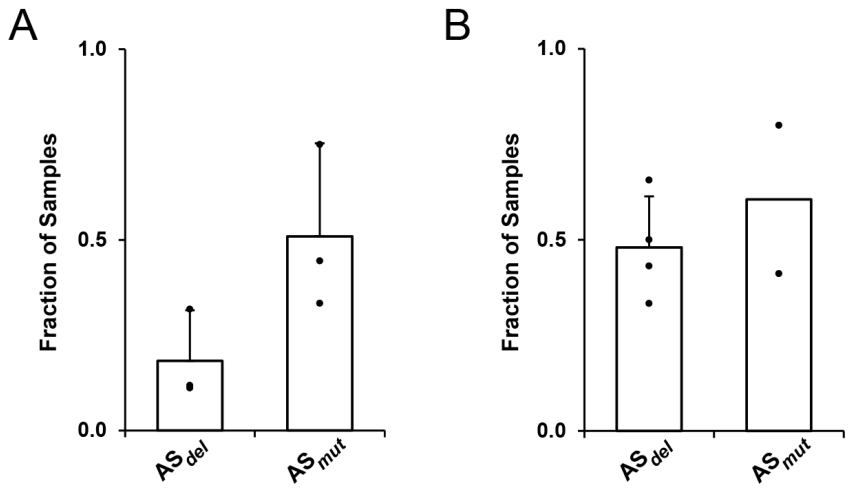

Supplementary Figure S6. Additional data for the ChP morphology using Angelman Syndrome-patient derived cell lines. (A) Total fraction of 3 week old AS_{del} and AS_{mut} whole brain organoids that have ChP morphology (fluid-filled cysts and sinuous). n = 3 independent organoid batches each with ≥ 9 organoids per genotype. (B) Total fraction of 5 week old whole brain organoids that have ChP morphology (fluid-filled cysts and sinuous). n=2 for AS_{mut} and n=4 for AS_{del} independent organoid batches each with ≥ 12 organoids per genotype. ChP: choroid plexus. Error bars are 95% confidence intervals. Error bars are not provided for samples with n<3.

Supplementary Table S1. *UBE3A* expression in human ChP tissue database information.

Database	Developing or Adult Brain
Allen Brain Atlas[88]	Adult brain
Allen Brain Atlas[88]	Developing brain
Human Protein Atlas[89]	Adult brain

Supplementary Table S2. Primary antibodies used in immunostaining experiments.

Antigen	Host	Supplier	Cat. No.	RRID	Dilution
SOX2	Goat	R&D Systems	AF2018	AB_355110	1:20
UBE3A	Rabbit	Bethyl Laboratories	A300-351A	AB_185563	1:250
pVimentin	Mouse	MBL International	D076-3S	AB_592962	1:200
MAP2	Mouse	Millipore Sigma	M1406	AB_477171	1:250
MAP2	Chicken	Abcam	AB92434	AB_2138147	1:300
TTR	Sheep	BIO-RAD	AHP1837	AB_2212089	1:100
EMX1	Rabbit	Atlas Antibodies	HPA006421	AB_1078739	1:50
Ki-67	Rabbit	Abcam	AB15580	AB_443209	1:800
Caspase-3	Rabbit	R&D Systems	AF835	AB_2243952	1:20
p16INK4a	Mouse	Abcam	AB54210	AB_881819	1:1000
CTIP2	Rat	Abcam	AB18465	AB_2064130	1:100
SATB2	Mouse	Abcam	AB51502	AB_882455	1:100
GLI3	Goat	R&D Systems	AF3690	AB_2232499	1:200

Supplementary Table S3. Software package information.

Name	Version
FlowJo Software[90]	v10.9.0
Salmon[91]	v1.7.0
Alevin-fry[92]	v0.5.0
Seurat[93]	v4.0.4
SCTransform[94]	v2
Speckle[95]	V1.2.0
zUMIs[96]	v2.9.4d
Samtools[97]	v1.10

Supplementary Data 1. Raw differential gene expression data related to Figure 3 (separate file).

Supplementary Data 2. Qiagen Ingenuity Pathway Analysis canonical pathways for 6 week organoids. Related to Figure 3 (separate file). Differentially expressed genes with false discovery rate $q < 0.05$, log2 (FC) $\geq |1|$ were used in this analysis.

Supplementary Data 3. Raw differential gene expression data related to Figure 5 and Supplemental Figure S3C (separate file).

Supplementary Data 4. Raw differential gene expression data related to Figure 6 (separate file).

Supplementary Data 5. Qiagen Ingenuity Pathway Analysis canonical pathways for 11 week organoids. Related to Figure 6 (separate file). Differentially expressed genes with false discovery rate $q < 0.05$, log2 (FC) $\geq |1|$ were used in this analysis.

Supplementary Data 6. Raw data related to figures (separate file).

Supplementary References

1. Pollen, A. A. *et al.* Molecular identity of human outer radial glia during cortical development. *Cell* **163**, 55–67 (2015).

2. Zeng, B. *et al.* The single-cell and spatial transcriptional landscape of human gastrulation and early brain development. *Cell Stem Cell* **30**, 851-866.e7 (2023).

3. Jourdon, A. *et al.* Modeling idiopathic autism in forebrain organoids reveals an imbalance of excitatory cortical neuron subtypes during early neurogenesis. *Nat. Neurosci.* **26**, 1505–1515 (2023).

4. Yao, Z. *et al.* A Single-Cell Roadmap of Lineage Bifurcation in Human ESC Models of Embryonic Brain Development. *Cell Stem Cell* **20**, (2017).

5. Camp, J. G. *et al.* Human cerebral organoids recapitulate gene expression programs of fetal neocortex development. *Proc. Natl. Acad. Sci. U. S. A.* **112**, 15672–15677 (2015).

6. Neely, M. D. *et al.* Single cell RNA sequencing detects persistent cell type- and methylmercury exposure paradigm-specific effects in a human cortical neurodevelopmental model. *Food Chem. Toxicol.* **154**, (2021).

7. Kanton, S. *et al.* Organoid single-cell genomic atlas uncovers human-specific features of brain development. *Nature* **574**, (2019).

8. Trujillo, C. A. *et al.* Complex Oscillatory Waves Emerging from Cortical Organoids Model Early Human Brain Network Development. *Cell Stem Cell* **25**, 558-569.e7 (2019).

9. van Bruggen, D. *et al.* Developmental landscape of human forebrain at a single-cell level identifies early waves of oligodendrogenesis. *Dev. Cell* **57**, 1421-1436.e5 (2022).

10. Fame, R. M., MacDonald, J. L. & Macklis, J. D. Development, specification, and diversity of callosal projection neurons. *Trends Neurosci.* **34**, 41–50 (2011).

11. Velasco, S. *et al.* Individual brain organoids reproducibly form cell diversity of the human cerebral cortex. *Nature* **570**, 523–527 (2019).

12. Polioudakis, D. *et al.* A Single-Cell Transcriptomic Atlas of Human Neocortical Development during Mid-gestation. *Neuron* **103**, 785-801.e8 (2019).

13. Dong, J. *et al.* Single-cell RNA-seq analysis unveils a prevalent epithelial/mesenchymal hybrid state during mouse organogenesis. *Genome Biol.* **19**, (2018).

14. Eze, U. C., Bhaduri, A., Haeussler, M., Nowakowski, T. J. & Kriegstein, A. R. Single-cell atlas of early human brain development highlights heterogeneity of human neuroepithelial cells and early radial glia. *Nat. Neurosci.* **24**, 584–594 (2021).

15. Li, X.-F. *et al.* Importance of K^+-dependent Na^+/Ca^{2+}-exchanger 2, NCKX2, in Motor Learning and Memory *. *J. Biol. Chem.* **281**, 6273–6282 (2006).

16. Stelzer, G. *et al.* The GeneCards Suite: From Gene Data Mining to Disease Genome Sequence Analyses. *Curr. Protoc. Bioinforma.* **54**, 1.30.1-1.30.33 (2016).

17. Safran, M. *et al.* The GeneCards Suite - Practical Guide to Life Science Databases. in (eds. Abugessaisa, I. & Kasukawa, T.) 27–56 (Springer Nature Singapore, 2021). doi:10.1007/978-981-16-5812-9_2.

18. The UniProt Consortium. UniProt: the Universal Protein Knowledgebase in 2023. *Nucleic Acids Res.* **51**, D523–D531 (2023).

19. The UniProt Consortium. UniProt: the Universal Protein Knowledgebase in 2025. *Nucleic Acids Res.* **53**, D609–D617 (2025).

20. Izawa, I., Nishizawa, M., Ohtakara, K. & Inagaki, M. Densin-180 Interacts with delta-Catenin/Neural Plakophilin-related Armadillo Repeat Protein at Synapses. *J. Biol. Chem.* **277**, 5345–5350 (2002).

21. Cho, C. H. *et al.* ANKS1B encoded AIDA-1 regulates social behaviors by controlling oligodendrocyte function. *Nat. Commun.* **14**, 8499 (2023).

22. Wang, F., Eagleson, K. L. & Levitt, P. Positive regulation of neocortical synapse formation by the Plexin-D1 receptor. *Brain Res.* **1616**, 157–165 (2015).

23. Sinning, A., Liebmann, L. & Hübner, C. A. Disruption of Slc4a10 augments neuronal excitability and modulates synaptic short-term plasticity. *Front. Cell. Neurosci.* **9**, 223 (2015).

24. Sinha, R. *et al.* LRRTM4: A Novel Regulator of Presynaptic Inhibition and Ribbon Synapse Arrangements of Retinal Bipolar Cells. *Neuron* **105**, 1007-1017.e5 (2020).

25. Schroeder, B. C., Hechenberger, M., Weinreich, F., Kubisch, C. & Jentsch, T. J. KCNQ5, a Novel Potassium Channel Broadly Expressed in Brain, Mediates M-type Currents*. *J. Biol. Chem.* **275**, 24089–24095 (2000).

26. Wu, Y. *et al.* Mutations in ionotropic AMPA receptor 3 alter channel properties and are associated with moderate cognitive impairment in humans. *Proc. Natl. Acad. Sci.* **104**, 18163–18168 (2007).

27. Gutierrez-Castellanos, N. *et al.* Motor Learning Requires Purkinje Cell Synaptic Potentiation through Activation of AMPA-Receptor Subunit GluA3. *Neuron* **93**, 409–424 (2017).

28. Andrásfalvy, B. K., Smith, M. A., Borchardt, T., Sprengel, R. & Magee, J. C. Impaired regulation of synaptic strength in hippocampal neurons from GluR1-deficient mice. *J. Physiol.* **552**, 35–45 (2003).

29. Rasmussen, A. H., Rasmussen, H. B. & Silahtaroglu, A. The DLGAP family: neuronal expression, function and role in brain disorders. *Mol. Brain* **10**, 43 (2017).

30. Helbig, K. L. *et al.* De Novo Pathogenic Variants in CACNA1E Cause Developmental and Epileptic Encephalopathy with Contractures, Macrocephaly, and Dyskinesias. *Am. J. Hum. Genet.* **103**, 666–678 (2018).

31. Cao, J. K., Kaplan, J. & Stella, N. ABHD6: Its Place in Endocannabinoid Signaling and Beyond. *Trends Pharmacol. Sci.* **40**, 267–277 (2019).

32. Wei, M. *et al.* α/β-Hydrolase domain-containing 6 (ABHD6) negatively regulates the surface delivery and synaptic function of AMPA receptors. *Proc. Natl. Acad. Sci. U. S. A.* **113**, E2695-704 (2016).

33. Mechaussier, S. *et al.* Loss of Function of RIMS2 Causes a Syndromic Congenital Cone-Rod Synaptic Disease with Neurodevelopmental and Pancreatic Involvement. *Am. J. Hum. Genet.* **106**, 859–871 (2020).

34. Acuna, C., Liu, X. & Südhof, T. C. How to Make an Active Zone: Unexpected Universal Functional Redundancy between RIMs and RIM-BPs. *Neuron* **91**, 792–807 (2016).

35. Gebhart, M. *et al.* Modulation of Cav1.3 Ca2+ channel gating by Rab3 interacting molecule. *Mol. Cell. Neurosci.* **44**, 246–259 (2010).

36. Li, X. *et al.* Aberrant methylation in neurofunctional gene serves as a hallmark of tumorigenesis and progression in colorectal cancer. *BMC Cancer* **23**, 315 (2023).

37. Matsumoto, A. *et al.* LIN7A depletion disrupts cerebral cortex development, contributing to intellectual disability in 12q21-deletion syndrome. *PLoS One* **9**, e92695 (2014).

38. Cooper, M. A., Crockett, D. P., Nowakowski, R. S., Gale, N. W. & Zhou, R. Distribution of EphA5 receptor protein in the developing and adult mouse nervous system. *J. Comp. Neurol.* **514**, 310–328 (2009).

39. Akaneya, Y. *et al.* Ephrin-A5 and EphA5 interaction induces synaptogenesis during early hippocampal development. *PLoS One* **5**, e12486 (2010).

40. Rochon, P.-L., Theriault, C., Rangel Olguin, A. G. & Krishnaswamy, A. The cell adhesion molecule Sdk1 shapes assembly of a retinal circuit that detects localized edges. *eLife* **10**, (2021).

41. Yamagata, M. & Sanes, J. R. Dscam and Sidekick proteins direct lamina-specific synaptic connections in vertebrate retina. *Nature* **451**, 465–469 (2008).

42. Yamagata, M., Weiner, J. A. & Sanes, J. R. Sidekicks: Synaptic Adhesion Molecules that Promote Lamina-Specific Connectivity in the Retina. *Cell* **110**, 649–660 (2002).

43. Kumar, A. *et al.* Neuronal Actin Dynamics, Spine Density and Neuronal Dendritic Complexity Are Regulated by CAP2. *Frontiers in Cellular Neuroscience* vol. 10 (2016).

44. Pelucchi, S. *et al.* Cyclase-associated protein 2 dimerization regulates cofilin in synaptic plasticity and Alzheimer's disease. *Brain Commun.* **2**, fcaa086 (2020).

45. Chen, Y.-K., Chen, C.-Y., Hu, H.-T. & Hsueh, Y.-P. CTTNBP2, but not CTTNBP2NL, regulates dendritic spinogenesis and synaptic distribution of the striatin-PP2A complex. *Mol. Biol. Cell* **23**, 4383–4392 (2012).

46. Shih, P.-Y. *et al.* CTTNBP2 Controls Synaptic Expression of Zinc-Related Autism-Associated Proteins and Regulates Synapse Formation and Autism-like Behaviors. *Cell Rep.* **31**, 107700 (2020).

47. Yamagishi, S. *et al.* FLRT2 and FLRT3 act as repulsive guidance cues for Unc5-positive

neurons. *EMBO J.* **30**, 2920–2933 (2011).

48. Cicvaric, A. *et al.* Enhanced synaptic plasticity and spatial memory in female but not male FLRT2-haplodeficient mice. *Sci. Rep.* **8**, 3703 (2018).

49. Seiradake, E. *et al.* FLRT structure: balancing repulsion and cell adhesion in cortical and vascular development. *Neuron* **84**, 370–385 (2014).

50. O'Dell, R. S. *et al.* Layer 6 cortical neurons require Reelin-Dab1 signaling for cellular orientation, Golgi deployment, and directed neurite growth into the marginal zone. *Neural Dev.* **7**, 25 (2012).

51. Hammond, V., Howell, B., Godinho, L. & Tan, S. S. disabled-1 functions cell autonomously during radial migration and cortical layering of pyramidal neurons. *J. Neurosci. Off. J. Soc. Neurosci.* **21**, 8798–8808 (2001).

52. Trotter, J. *et al.* Dab1 is required for synaptic plasticity and associative learning. *J. Neurosci. Off. J. Soc. Neurosci.* **33**, 15652–15668 (2013).

53. Gene [Internet]. Bethesda (MD): National Library of Medicine (US), National Center for Biotechnology Information; 2004. https://www.ncbi.nlm.nih.gov/gene/.

54. Miller, A. C., Voelker, L. H., Shah, A. N. & Moens, C. B. Neurobeachin is required postsynaptically for electrical and chemical synapse formation. *Curr. Biol.* **25**, 16–28 (2015).

55. Nair, R. *et al.* Neurobeachin regulates neurotransmitter receptor trafficking to synapses. *J. Cell Biol.* **200**, 61–80 (2013).

56. Wang, X. *et al.* Neurobeachin: A protein kinase A-anchoring, beige/Chediak-higashi protein homolog implicated in neuronal membrane traffic. *J. Neurosci. Off. J. Soc. Neurosci.* **20**, 8551–8565 (2000).

57. Kim, H. R. *et al.* NELL2 Function in Axon Development of Hippocampal Neurons. *Mol. Cells* **43**, 581–589 (2020).

58. Betancourt, J., Katzman, S. & Chen, B. Nuclear factor one B regulates neural stem cell differentiation and axonal projection of corticofugal neurons. *J. Comp. Neurol.* **522**, 6–35 (2014).

59. Liu, Y. *et al.* Myosin Vb controls biogenesis of post-Golgi Rab10 carriers during axon development. *Nat. Commun.* **4**, 2005 (2013).

60. Rehfeld, F. *et al.* The RNA-binding protein ARPP21 controls dendritic branching by functionally opposing the miRNA it hosts. *Nat. Commun.* **9**, 1235 (2018).

61. Leonard, C. E., Baydyuk, M., Stepler, M. A., Burton, D. A. & Donoghue, M. J. EphA7 isoforms differentially regulate cortical dendrite development. *PLoS One* **15**, e0231561 (2020).

62. Clifford, M. A. *et al.* EphA7 signaling guides cortical dendritic development and spine maturation. *Proc. Natl. Acad. Sci.* **111**, 4994–4999 (2014).

63. Villanueva, A. A. *et al.* The Netrin-4/ Neogenin-1 axis promotes neuroblastoma cell survival and migration. *Oncotarget* **8**, 9767–9782 (2017).

64. Emerson, S. E., Stergas, H. R., Bupp-Chickering, S. O. & Ebert, A. M. Shootin-1 is required for nervous system development in zebrafish. *Dev. Dyn. an Off. Publ. Am. Assoc. Anat.* **249**, 1285–1295 (2020).

65. Zhang, M. *et al.* Axonogenesis Is Coordinated by Neuron-Specific Alternative Splicing Programming and Splicing Regulator PTBP2. *Neuron* **101**, 690-706.e10 (2019).

66. Ergin, V., Erdogan, M. & Menevse, A. Regulation of Shootin1 Gene Expression Involves NGF-induced Alternative Splicing during Neuronal Differentiation of PC12 Cells. *Sci. Rep.* **5**, 17931 (2015).

67. Lucas, B. & Hardin, J. Mind the (sr)GAP - roles of Slit-Robo GAPs in neurons, brains and beyond. *J. Cell Sci.* **130**, 3965–3974 (2017).

68. Kwan, K. Y. *et al.* SOX5 postmitotically regulates migration, postmigratory differentiation, and projections of subplate and deep-layer neocortical neurons. *Proc. Natl. Acad. Sci. U. S. A.* **105**, 16021–16026 (2008).

69. Moore, J. M. *et al.* Laf4/Aff3, a gene involved in intellectual disability, is required for cellular migration in the mouse cerebral cortex. *PLoS One* **9**, e105933 (2014).

70. Wiegreffe, C. *et al.* Bcl11a (Ctip1) Controls Migration of Cortical Projection Neurons through Regulation of Sema3c. *Neuron* **87**, 311–325 (2015).

71. Cohen, J. S. *et al.* Further evidence that de novo missense and truncating variants in ZBTB18 cause intellectual disability with variable features. *Clin. Genet.* **91**, 697–707 (2017).

72. Wang, R. *et al.* ZBTB18 restricts chromatin accessibility and prevents transcriptional adaptations that drive metastasis. *Sci. Adv.* **9**, eabq3951 (2023).

73. Whitehouse, C. *et al.* A transfected sialyltransferase that is elevated in breast cancer and localizes to the medial/trans-Golgi apparatus inhibits the development of core-2-based O-glycans. *J. Cell Biol.* **137**, 1229–1241 (1997).

74. Steiner, A. *et al.* Deficiency in coatomer complex I causes aberrant activation of STING signalling. *Nat. Commun.* **13**, 2321 (2022).

75. Michibata, H., Yanaka, N., Kanoh, Y., Okumura, K. & Omori, K. Human Ca2+/calmodulin-dependent phosphodiesterase PDE1A: novel splice variants, their specific expression, genomic organization, and chromosomal localization. *Biochim. Biophys. Acta - Gene Struct. Expr.* **1517**, 278–287 (2001).

76. Sue, M. *et al.* Thyroglobulin (Tg) activates MAPK pathway to induce thyroid cell growth in the absence of TSH, insulin and serum. *Biochem. Biophys. Res. Commun.* **420**, 611–615 (2012).

77. Nishino, T. *et al.* GAREM1 is involved in controlling body mass in mice and humans. *Biochem. Biophys. Res. Commun.* **628**, 91–97 (2022).

78. Tashiro, K. *et al.* GAREM, a Novel Adaptor Protein for Growth Factor Receptor-bound Protein 2, Contributes to Cellular Transformation through the Activation of Extracellular Signal-regulated Kinase Signaling*. *J. Biol. Chem.* **284**, 20206–20214 (2009).

79. Yao, H. *et al.* CHD7 promotes neural progenitor differentiation in embryonic stem cells via altered chromatin accessibility and nascent gene expression. *Sci. Rep.* **10**, 17445 (2020).

80. Hemmi, K. *et al.* A homeodomain-zinc finger protein, ZFHX4, is expressed in neuronal differentiation manner and suppressed in muscle differentiation manner. *Biol. Pharm. Bull.* **29**, 1830–1835 (2006).

81. Hamada, T. *et al.* The expression of SCDGF/PDGF-C/fallotein and SCDGF-B/PDGF-D in the rat central nervous system. *Mech. Dev.* **112**, 161–164 (2002).

82. Tian, Y., Zhan, Y., Jiang, Q., Lu, W. & Li, X. Expression and function of PDGF-C in development and stem cells. *Open Biol.* **11**, 210268 (2021).

83. Ogino, H. *et al.* Secreted Metalloproteinase ADAMTS-3 Inactivates Reelin. *J. Neurosci. Off. J. Soc. Neurosci.* **37**, 3181–3191 (2017).

84. Büttner, N., Johnsen, S. A., Kügler, S. & Vogel, T. Af9/Mllt3 interferes with Tbr1 expression through epigenetic modification of histone H3K79 during development of the cerebral cortex. *Proc. Natl. Acad. Sci. U. S. A.* **107**, 7042–7047 (2010).

85. Kumamoto, T. & Hanashima, C. Neuronal subtype specification in establishing mammalian neocortical circuits. *Neurosci. Res.* **86**, 37–49 (2014).

86. Castiglioni, V. *et al.* Dynamic and Cell-Specific DACH1 Expression in Human Neocortical and Striatal Development. *Cereb. Cortex* **29**, 2115–2124 (2019).

87. Rottkamp, C. A., Lobur, K. J., Wladyka, C. L., Lucky, A. K. & O'Gorman, S. Pbx3 is required for normal locomotion and dorsal horn development. *Dev. Biol.* **314**, 23–39 (2008).

88. Sunkin, S. M. *et al.* Allen Brain Atlas: An integrated spatio-temporal portal for exploring the central nervous system. *Nucleic Acids Res.* **41**, (2013).

89. Pontén, F., Jirström, K. & Uhlen, M. The Human Protein Atlas - A tool for pathology. *Journal of Pathology* vol. 216 (2008).

90. FlowJo™ Software (for Windows), v10.9.0. Ashland, OR: Becton, Dickinson and Company; 2023.

91. Patro, R., Duggal, G., Love, M. I., Irizarry, R. A. & Kingsford, C. Salmon: fast and bias-aware quantification of transcript expression using dual-phase inference. *Nat. Methods* **14**, (2017).

92. He, D. *et al.* Alevin-fry unlocks rapid, accurate and memory-frugal quantification of single-cell RNA-seq data. *Nat. Methods* **19**, (2022).

93. Butler, A., Hoffman, P., Smibert, P., Papalexi, E. & Satija, R. Integrating single-cell transcriptomic data across different conditions, technologies, and species. *Nat. Biotechnol.*

36, 411–420 (2018).

94. Hafemeister, C. & Satija, R. Normalization and variance stabilization of single-cell RNA-seq data using regularized negative binomial regression. *Genome Biol.* **20**, (2019).

95. Phipson, B. *et al.* propeller: testing for differences in cell type proportions in single cell data. *Bioinformatics* **38**, (2022).

96. Parekh, S., Ziegenhain, C., Vieth, B., Enard, W. & Hellmann, I. zUMIs - A fast and flexible pipeline to process RNA sequencing data with UMIs. *Gigascience* **7**, 1–9 (2018).

97. Li, H. *et al.* The Sequence Alignment/Map format and SAMtools. *Bioinformatics* **25**, (2009).